geosciences

MDPI

Article

Velocity Model Construction and Time-to-Depth Conversion of a Vintage Seismic Reflection Profile for Improving the Constraints on a Subsurface Geological Model: An Example from the Sicily Channel (Central Mediterranean Sea)

Aasiya Qadir [1,*], Nicolò Chizzini [1], Mariagiada Maiorana [2], Andrea Artoni [1], Luigi Torelli [1] and Attilio Sulli [2]

[1] Department of Chemistry, Life Sciences and Environmental Sustainability, University of Parma, Parco Area Delle Scienze, 157/A, 43124 Parma, Italy; nicolo.chizzini@unipr.it (N.C.); andrea.artoni@unipr.it (A.A.); luigi.torelli@unipr.it (L.T.)

[2] Department of Earth and Marine Sciences, University of Palermo, Via Archirafi, 22, 90123 Palermo, Italy; mariagiada.maiorana@unipa.it (M.M.); attilio.sulli@unipa.it (A.S.)

* Correspondence: aasiya.qadir@unipr.it

Abstract: The well-known uncertainties in subsurface velocity field definition call for the integration of all the available data, including vintage seismic profiles, which, despite typically being in raster or paper format, often contain velocities derived from stacking and associated interval velocities. This study aims to build a velocity model for the time-to-depth conversion of an interpreted seismic reflection profile by using the interval velocity reported on a vintage, paper-format seismic profile and contribute to improving the subsurface geological model of the Sicily Channel, Central Mediterranean. Spline interpolation is used for velocity model building of the shallower part (3.5 sec TWT) of the seismic profile CS89-01, derived from the stacking velocities of 31 Common Depth Point (CDP) gathers. This was followed by the Gaussian convolution operator and a data exclusion filter to improve the accuracy of the velocity model. The time-to-depth-converted seismic reflection profile is a regional cross-section that covers almost the entire Sicily Channel, crossing part of the northern margin of the African Plate, from Tunisia to eastern Sicily. This study provides a new subsurface velocity field that can be applied, or taken into account, to most parts of the Sicily Channel when structural and stratigraphic interpretations are carried out at specific sites and where uncertainties in subsurface geological model exist (e.g., in the present study, the volcanic bodies in the Pantelleria Graben and Lampedusa High).

Keywords: velocity model; time-to-depth conversion; interval velocities; vintage seismic profiles; Sicily Channel

Academic Editor: Ioannis Koukouvelas

Received: 27 February 2025
Revised: 18 March 2025
Accepted: 19 March 2025
Published: 23 March 2025

Citation: Qadir, A.; Chizzini, N.; Maiorana, M.; Artoni, A.; Torelli, L.; Sulli, A. Velocity Model Construction and Time-to-Depth Conversion of a Vintage Seismic Reflection Profile for Improving the Constraints on a Subsurface Geological Model: An Example from the Sicily Channel (Central Mediterranean Sea). *Geosciences* **2025**, *15*, 114. https://doi.org/10.3390/geosciences15040114

1. Introduction

The increasing number of public web-databases (e.g., for Italy, ViDEPI, https://www.videpi.com (accessed on 18 March 2025); SNAP, https://snap.ogs.trieste.it (accessed on 18 March 2025)) and archives of research institutions that contain images of seismic reflection profiles printed on paper and/or scanned in raster format provide valuable information on the subsurface geology of different areas [1–4]. This increase in the public accessibility of vintage seismic profiles is consequential to the decline in the demand for the acquisition of new seismic reflection surveys and the advancements in the acquisition and processing techniques that generate higher-quality images; the latter are often unavailable to the public. Nonetheless, these data are crucial for studying subsurface geology at various depths,

providing essential information for water, hydrocarbon, and raw materials exploration, geohazard analysis, and geothermal field planning.

Seismic profiles characterized by a broad geographical extension, [1,5] acquired and processed between the 1960s and 1990s, are now widely available and potentially represent the only public repository of subsurface data in some areas (e.g., ViDEPI database). These vintage profiles are crucial for geoscience research, as modern high-resolution subsurface datasets are expensive and not accessible to the public. They help researchers to understand a region's tectonic and geological history and can be used for earthquake and geohazard studies [6–8]. Many vintage seismic reflection profiles are often in paper format, with most public databases (e.g., ViDEPI website) providing scanned pdf-format profiles. However, seismic profiles in time do not provide a comprehensive understanding of subsurface features, as they represent an altered image of the geometries of the subsurface geological bodies [9–13]. Time-to-depth conversion of seismic horizons and faults through detailed velocity models is an essential way to improve the accuracy of the subsurface stratigraphy and structural features, which is executed by using interval velocities [9,14–16]. The interval velocities provide the average speed of seismic waves traveling through the layers between two stratigraphic horizons, making them suitable for our analysis. The velocity model is essential for effective resource management and hazard assessments while planning for drilling or exploration [15]. It improves the effectiveness of kinematic models in understanding fault mechanics and structural evolution, leading to improved decision-making in hydrocarbon exploration and other geological assessments [14,17].

Seismic profiles or their interpretation (most recent non-vintage profiles) in digital format are easy to convert into depth and can be analyzed using dedicated software (e.g., IHS Kingdom of S&P, Decision Space suite of Landmark, PetrelTM of Schlumberger, Oasis Montaj of Geosoft, MOVE suite of Petex), but the maintenance, licensing, and specialized functionality costs make them expensive to use for the public and small companies. Because of these reasons, vintage seismic reflection profiles have recently received particular attention [8,18,19]. Therefore, the main objective of this work is to develop velocity models derived from the velocities reported in vintage seismic profiles to convert seismic horizons and faults into depth for a specific case study: the Sicily Channel in the Central Mediterranean Sea. The velocity models involve the use of interpolation tests (i.e., Kriging, Inverse Distance Weighted (IDW), and spline) and smoothing techniques (i.e., Gaussian low-pass filter and data exclusion filter) to achieve good results. The velocity field was calculated for vintage seismic profile CS89-01 scanned from a paper format version. It was converted from time to depth for the first time, and it contributed to better constraining the subsurface geological model of the Sicily Channel, which has recently received attention for CCS [20], and it is an area favorable for geothermal energy sources due to recent active volcanism [21,22]. In addition, velocity models of the Sicily Channel exist in the literature [23,24], but they focus on the deeper parts, the crust and mantle, while the velocity models obtained in this study focus on the shallower part (down to $\approx$ 6 km depth).

The CS89-01 profile crosses the Sicily Channel (Central Mediterranean Sea) from SSE to NNW, highlighting the stratigraphic and structural setting of the area at a regional scale and across various basins and sub-basins (Figure 1). Like many vintage seismic profiles, this is a scanned paper copy not available in digital format in any database, but it contains the complete suite of stacking velocities (Figure 2a–c) (for a detailed list of velocities, refer to Supplementary Material S1). Furthermore, this portion of the seismic profile is well known in the literature (Figure 2a'–c'; [25–27]). For the first time, its seismic interpretation is converted to depth from time, providing new insights into the geological setting down to 6 km depth in this sector of the Sicily Channel, which was intensively investigated in the past and recently [28–37].

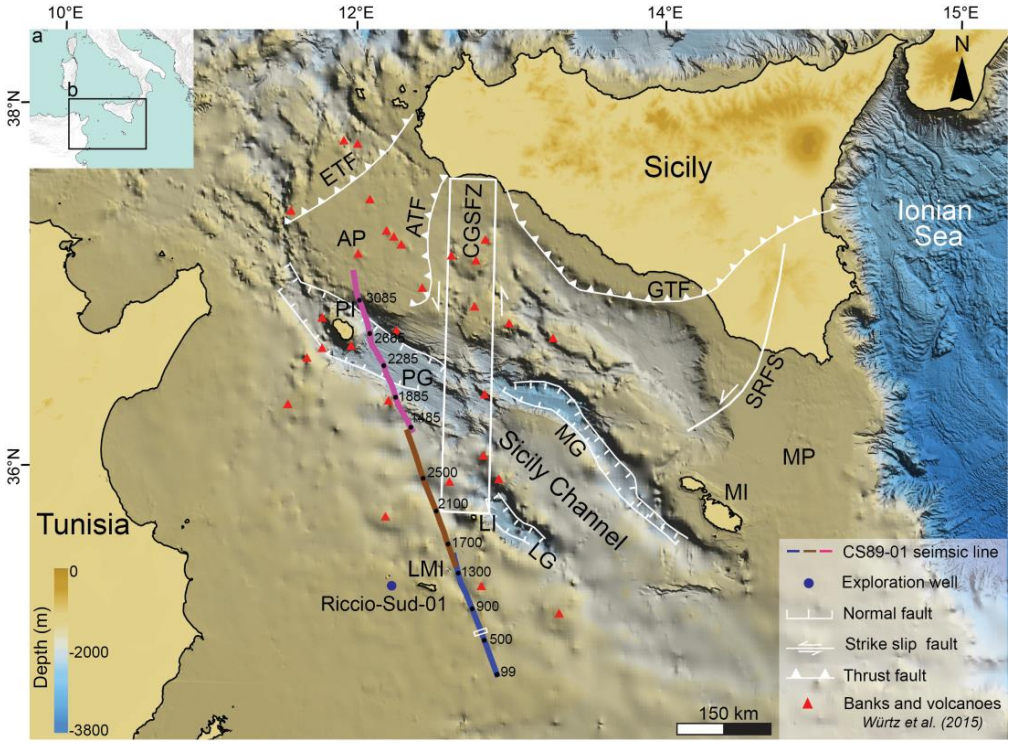

Figure 1. (a) Study area location; (b) structural map of Sicily Channel and the position of Riccio Sud-01 exploration well and multichannel seismic reflection profile CS89-01 (after [25–27]). Bathymetry data extracted from EMODnet (http://www.emodnet-bathymetry.eu/ (accessed on 18 March 2025)) DTM (2022). The white rectangle on the line between shot points 500 and 900 displays the position where the well is calibrated, with the depth converted to stratigraphic units. The main structural features are modified from [36]. AP: Adventure Plateau. ATF: Adventure Thrust Fault. CGSFZ: Capo Granitola–Sciacca Fault Zone. ETF: Egadi Thrust Fault. GTF: Gela Thrust Front. LG: Linosa Graben. LMI: Lampedusa Island. LI: Linosa Island. MG: Malta Graben. MI: Malta Island, PG: Pantelleria Graben. PI: Pantelleria Island. SRFS: Scicli–Ragusa Fault System.

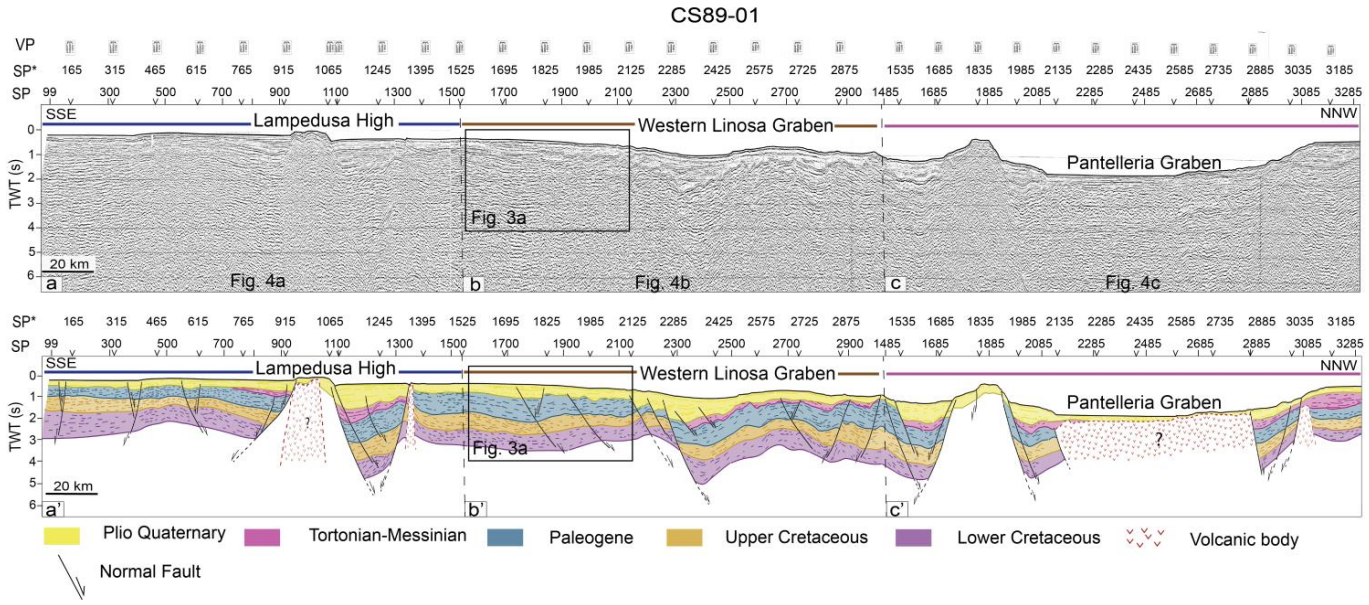

Figure 2. (**a**–**c**) Uninterpreted and (**a′**–**c′**) interpreted parts of multichannel seismic reflection profile CS89-01 (after [25–27]) considered for velocity modeling. The Lampedusa High is flanked by a listric

fault (approximately between shot points 700 and 900), the Western Linosa Graben located along SSE-NNW direction is flanked by an NNW-trending major planar normal fault approximately between shot points 2100 and 2300, and the Pantelleria Graben is intruded by the volcanic body. SPs: shot points. SP*: shot points corresponding to the position of the Common Depth Point (CDP) gathers on which the velocity analysis was performed in 1989. ?: uncertainty of volcanic body. VP: Velocity panels corresponding to respective position (v) on the image along which the stacking was done (for detail of velocity panels refer to Supplementary Material S1). The highlighted portions of (**b**,**b′**) were considered for the representation of the methodology.

2. Brief Geological Framework of the Study Area

The SE-NW-oriented Sicily Channel (Figure 1) is strictly related to the convergence of African and Eurasian plates in the Neogene, which played a significant role in the tectonic evolution of the Central Mediterranean region [38–43]. The Sicily Channel was developed and shaped by two geodynamic processes: the Neogene formation of the Sicilian–Maghrebian Chain and Early Pliocene rifting [26,30,32,42,44–47]. This Pliocene rifting phase paved the way for the formation of the most prominent NW-trending Pantelleria, Linosa, and Malta grabens (Figure 1; [28–36]. The largest Pantelleria Graben [35,36] is separated from the Linosa and Malta grabens by the Capo Granitola–Sciacca Fault Zone (CGSFZ), a wide N-S-oriented transfer zone that originated in the Lower Pliocene and is characterized by a left-kinematic movement, featuring shallow banks that exhibit the presence of volcanic bodies (Figure 1; [29,45,48–52]). Plio-Pleistocene rift-related volcanism evidence is preserved in the Pantelleria and Linosa islands [28,30–39,49,53–55].

Sicily Channel succession consists of a thick crystalline basement [24,36,56,57] overlain by a Triassic to Jurassic platform carbonate unit followed up by Lower Cretaceous and Upper Cretaceous to Eocene successions, consisting of limestones with intercalations of marls and clay [31,32,35,36,51]. The Upper Miocene (Tortonian to Messinian) siliciclastic deposits can be found in the deeper parts of the Neogene basins of the Lampedusa shelf [26,58,59]. Finally, the sequence culminates with Plio-Quaternary clayey sediments [26,35,36,51,60].

3. Materials

The 235 km long multi-channel seismic reflection line CS89-01 was acquired by the Institute of Marine Sciences of the National Research Council of Italy (CNR-ISMAR) in 1989 and is now available only in paper copy. The acquired data were recorded on magnetic tape in a format that cannot be read anymore. It extends across the Sicily Channel in the SSE–NNW direction (Figures 1 and 2).

The seismic horizons and faults marked on the CS89-01 time profile by Torelli et al. (1991, 1995) [25,26] and Argnani and Torelli (2001) [27] were converted to depth from the time domain using the given interval velocities. The original seismic section has been subjected to migration, which is a crucial step in refining the seismic data. The ages of the stratigraphic units are based on the data from the Riccio-Sud-01 well located 60 km away from the line and the literature, mainly Torelli et al. (1991, 1995) [25,26]. The acquisition parameters and processing steps for obtaining the seismic reflection profiles in TWT are listed in Table 1. The interval velocity data for time-to-depth conversion were extracted from 31 Common Depth Point (CDP) gathers reported on the header of the profile (Figure 2a–c); the interval velocities of these CDP gathers are available in Supplementary Material S1. The interval velocities represent true seismic wave velocities, which are essential for transforming seismic data into meaningful geological interpretations [61].

Table 1. Acquisition parameters, geometry, and processing sequence of CS89-01 multichannel seismic reflection profile.

Acquisition Parameters		Acquisition Geometry		Processing	
Shot by	OGS*	Energy source	Air gun	Bination*	50/62 Hz
Vessel	OGS Explora	Source depth	6 m	Trace sum	Trace sum of two adjacent traces
Recorder	SERCEL SN-358	Streamer	2975 m	Velocity analysis	Stacking velocity
Sample rate	4 ms	Streamer depth	12 m	NMO correction	Application of NMO correction and mute
Field filters	Low 8 Hz High 77 Hz	Shot interval	50 m	Stack	3000%
Coverage	3000%	Groups interval	25 m	Filter	200ms zero-phase bandpass filter

OGS*: Osservatorio Geofisico Sperimentale, Trieste, Italy. Bination*: the technique of removing high-frequency components from seismic data before the sample is used to prevent aliasing, which occurs when data are sampled at too low a rate.

Line drawings of the seismic reflection profiles were generated with the graphics software Adobe Illustrator®, while ArcGIS was used for velocity gridding and interpolation method testing. Golden Surfer software was used for smoothing (Gaussian low-pass filter and data exclusion filter); the complete workflow is reported in Figure 3.

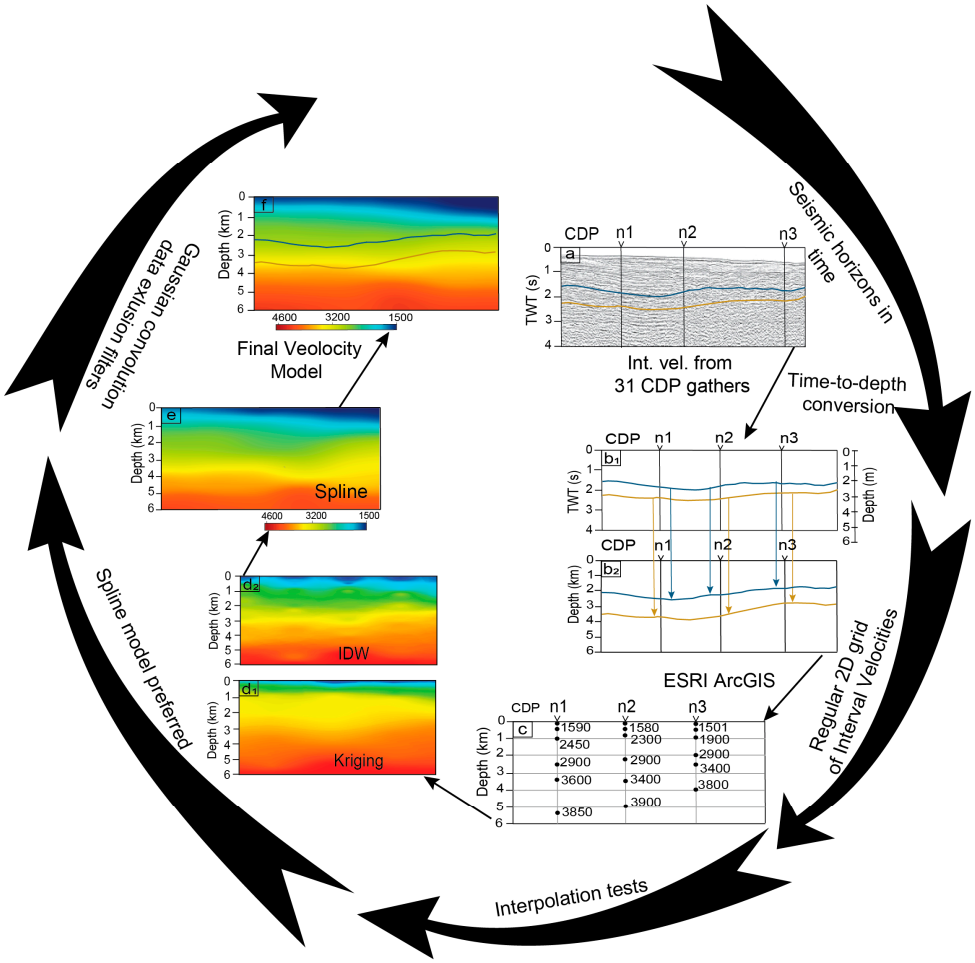

Figure 3. Workflow for the construction of velocity models and depth conversion of seismic horizons and faults from the interval velocities: (**a**) Part of the seismic profile representing the exact position

of stratigraphic horizons (yellow and blue) in time, highlighted in Figure 2b. (**b1**,**b2**) Show how the horizons are moved according to the calculated depth from the interval velocities (for the velocities associated with CDP n1, n2, and n3, refer to SP* 1695, 1825, 1985, respectively). (**c**) Interval velocity grid of (**a**) based on the data in Supplementary Material S2. (**d1**,**d2**) Velocity models generated by implementing Kriging and IDW interpolation. (**e**) Spline interpolation velocity model. (**f**) Velocity model achieved by the application of Gaussian Convolution and a data exclusion filter with the depth-converted horizons overlaid on it.

In this study, the interval velocities were taken from the boxes represented on the top of the profile (CDP gathers with interval velocities obtained from Dix's formula [62] in Figure 2a–c and Supplementary Material S1) to construct the velocity models and depth profile. As a representation of the methodology steps, we considered two seismic horizons (yellow base of Upper Cretaceous and blue base of Paleogene) and the interval velocities associated with a part of the profile highlighted in Figure 2b,b' with 3 CDP gathers (n1, n2, n3). We used the interval velocities from the seismic datum plane (0 m sea level corresponding to 0 sec TWT) down to the interpreted yellow and blue horizons (Figure 3a) to convert them to depth (Figure 3b1,b2,c).

4. Methods

The highlighted portion of Figure 2b was considered for the representation of the methodology (Figure 3a). The base of Paleogene and the base of Upper Cretaceous were converted to depth using the interval velocities between them (Figure 3b1,b2). The interval velocities were spatially arranged in a grid (Figure 3c) with respect to the depth of interpreted horizons (sea floor surface, base of Plio-Quaternary, base of Paleogene, base of Upper Cretaceous, and base of Lower Cretaceous); for the interval velocity values of CDP n1 (SP* 1695), n2 (SP* 1825), and n3 (SP* 1985), see the details in Supplementary Material S2. The gap of the velocity field of two adjacent vertical lines (corresponding to CDP positions) was filled with interpolated interval velocities. The spline interpolation model was considered in this study over the Kriging and IDW models (Figure 3d1,d2,e) because neither of these interpolation methods were suitable for generating good enough velocity models for further analysis. The spline interpolation models generated in this study using cubic polynomials (Degree 3) are smoother and more continuous than the models built using the IDW and Kriging methods (for details, see Supplementary Material S3). Spline interpolation is a powerful interpolation tool that uses a mathematical function to estimate the values and results in a model that connects the input data points in a pattern [63]. It effectively approximates a smooth curve through a set of data points [63–69].

The application of smoothing techniques enhances the quality of the initial velocity models by suppressing the unwanted noise; the proper adjustment of the control parameters of the smoothing techniques can make their performance more efficient. A Gaussian filter [70,71] and data exclusion filter [72] were used to improve the accuracy of the model (Figure 3e,f). A Gaussian convolution filter is a low-pass filter, and it suppressed the noise and emphasized the large-scale features in the model (Figure 3f; [73–76]). The Gaussian filter worked optimally and convolved the velocity model with a Gaussian function [70]. The below-mentioned Gaussian convolution mask coefficients were implemented in a 3×3 neighborhood on the model, which did not impact its overall intensity and quality.

$$\frac{1}{16} = \begin{bmatrix} 1 & 2 & 1 \\ 2 & 4 & 2 \\ 1 & 2 & 1 \end{bmatrix}$$

The application of the Gaussian convolution mask improved the velocity model to a greater extent. However, there still remained some incorrect velocities in the model,

which originated from the original velocity data. To remove the inconsistent velocities from the velocity model, the geology of the area along which the line passes was taken into consideration. The filter works with Boolean expressions [77] to specify the criteria to remove the inconsistent velocity components. The filter works on an already-saved grid that contains depth and velocity values as nodes; the inaccurate velocity data points were specified in the Data Exclusion filter text box for each model. The threshold was defined based on regional geological knowledge (especially lithology-based) and literature data [23,24], excluding the velocity values (specific velocity nodes) that were manually defined (based on depth and distance along a model) for exclusion and are inconsistent with expected lithologies (clay, marl, sand, and limestone) in the region within the depth range of 0–6 km. Thus, the velocity model was updated by eliminating error components by opting for the data exclusion filter (Figure 3f).

The depth profile was superimposed on the final velocity model (Figure 3f), which was useful to analyze the model in detail. For details of the interval velocity and depth in Figure 3f, refer to SP* 1685, 1825, and 1985 in Supplementary Material S2.

5. Results and Discussion

5.1. Velocity Analysis from Velocity Models for Uncertain Portion

In this study, the velocity modeling and time-to-depth conversion of the seismic interpretation of a vintage seismic reflection profile CS89-01 (Figures 1 and 2a–c) was performed, and three portions were given particularly attention for being representative of the main different geological features of the Sicily Channel (Figure 4).

In Lampedusa High (Figures 4 and 5a), there is uncertainty regarding volcanic bodies intruding the high or a carbonatic horst. There were similar uncertainties for Pantelleria Graben, where the evidence of buried magmatic bodies was finally defined [35,78]. The geological models defined along the CS89-01 profile reveal a broader range of velocity values from 1450 m/s to 4900 m/s around Lampedusa High (Figure 5). The velocity model (Figure 5a) does not feature high velocities at shallow depths, which is congruent with the absence of volcanic bodies in Lampedusa High.

The velocity models (Figures 4 and 5) are congruent with the velocities presented in Cassinis et al. (2003) [24] for the lines from different parts of the Sicily Channel, including Pantelleria Graben, which show that up to ~6 km depth the velocities rise to ~5 km/s. Figure 5a does not indicate high velocities at a shallow depth, although some igneous intrusions might occur along the profile. This may be due to the small scale of the volcanic body, which corresponds to the lack of intruding volcanic bodies in Lampedusa High. The antiform shape of the high-velocity contours at depth in the Pantelleria Graben (Figure 5c) confirms the occurrence of a volcanic body in the graben, as reported in previous works [28–36,53], which revealed a depleted tholeiitic signature derived from a shallow mantle source [49]. The positions of Linosa and Pantelleria indicate that Pleistocene to Holocene volcanism in the grabens of the Sicily Channel is concentrated at their NW limits, with the greatest magmatic flux at Pantelleria [35]. The volcanic complex in Pantelleria Graben is vast, with one prominent body that is roughly 46 km long and 20 km wide [36]. A history of notable volcanic eruptions is reflected in this complex, which consists of both emergent and submerged volcanic formations [55,79].

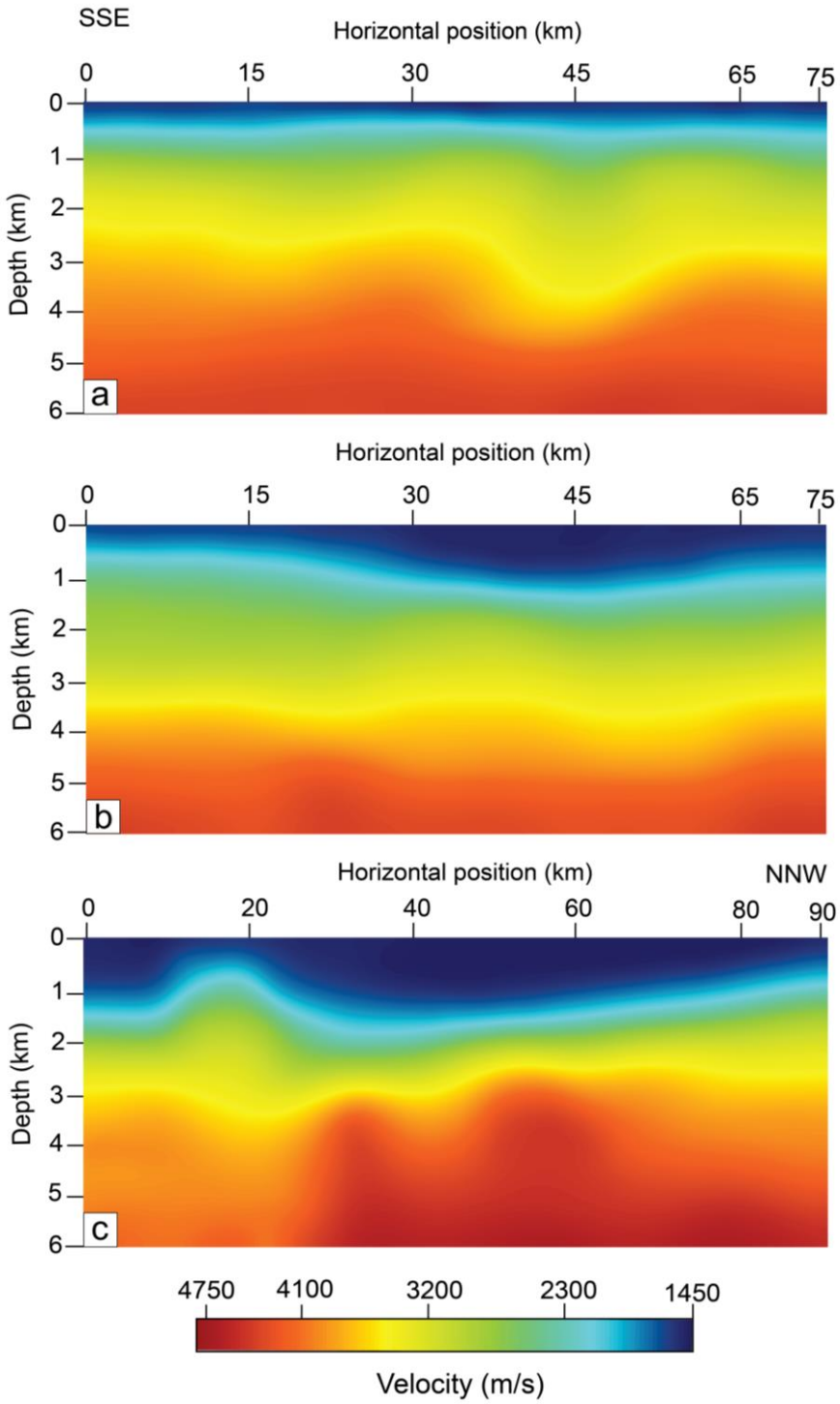

Figure 4. (**a**–**c**) Final velocity models after the application of the Gaussian convolution operator and data exclusion filter.

The seismic facies analysis also supports the presence of volcanic bodies in the graben. The velocity difference at various positions (i.e., ~2 km and ~39 km) at the same ~1 km depth in the velocity model (Figure 5b) may suggest contrasting sediment compaction levels or the abundance of clayey sediments of the Plio-Quaternary unit in the Western Linosa Graben [36,80].

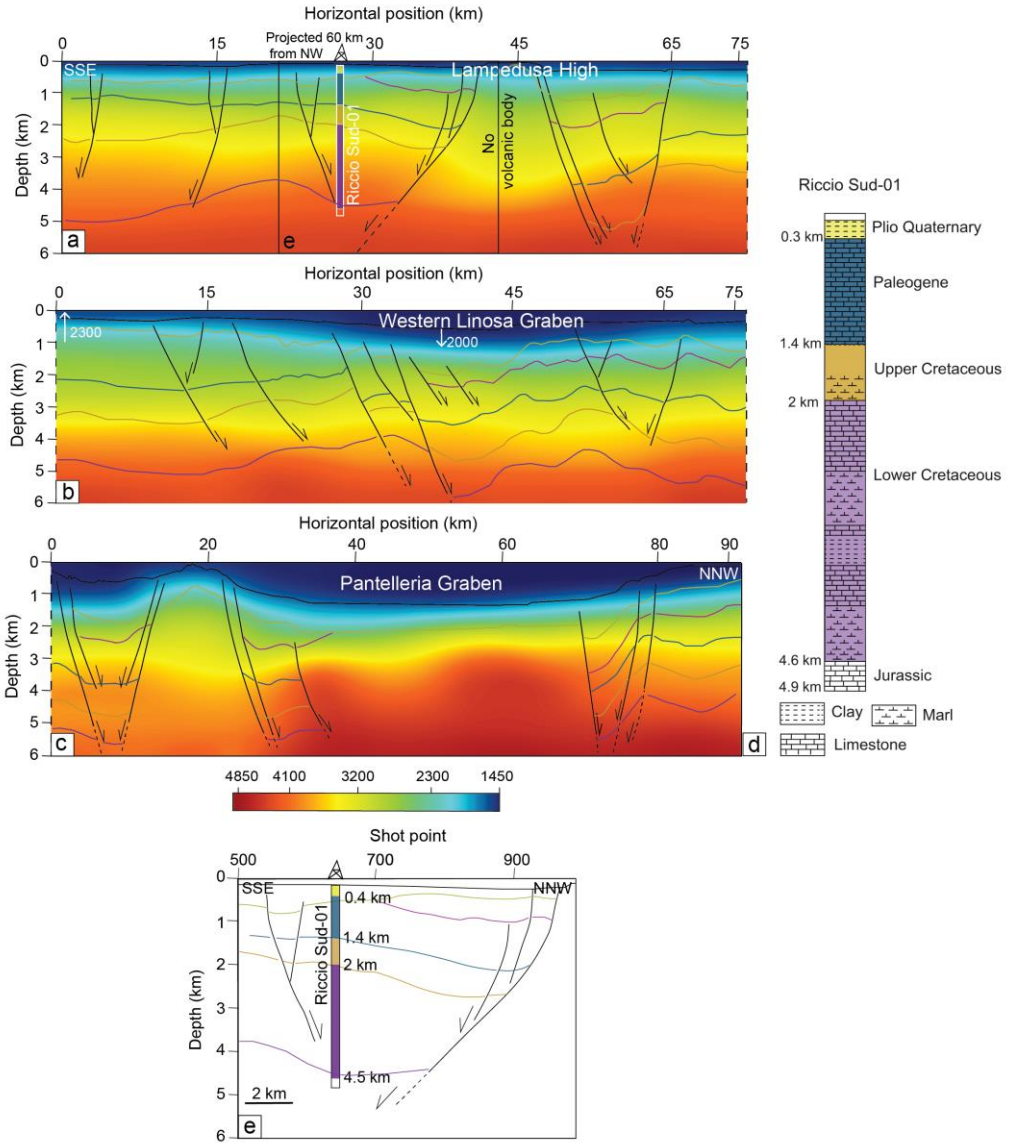

Figure 5. Depth-converted stratigraphic horizons and faults from velocity models overlaid over them. (**a**) No indication of the presence of a volcanic body in Lampedusa High and the calibration of the Riccio Sud-01 well. (**b**) Velocity contrast at a distance of ~2km and Western Linosa Graben at a depth of ~0.8 km. (**c**) Antiform shape of velocity contours between 20 km and 70 km may be evidence of the presence of a volcanic body in the Pantelleria Graben. (**d**) Stratigraphy of the Riccio Sud-01 well. (**e**) Magnified image from the depth profile (**a**) showing the stratigraphic units in good correspondence with the well data. (**d**) The depth values mentioned on the right side of the projected well in (**e**) indicate the depth of each horizon at that point achieved after depth conversion. See the location of the line in Figure 1 and refer to Figure 2 for the meaning of stratigraphic horizons and faults.

5.2. Time-to-Depth Conversion for Stratigraphic and Structural Analysis

The seismic horizons and the faults from the CS89-01 line (in time), which correspond to different geological contexts in the Sicily Channel, were converted to depth using the velocity models. Depth-converted stratigraphic horizons using the refined horizontal variation in the interval velocities (Supplementary Material S2) were overlaid on the velocity models (Figure 5a–c).

The Lampedusa shelf reveals a complex geological history characterized by significant structural features and sediment deposition over time [81]. Stratigraphy is heavily influenced by extensional tectonics [81], which has led to the formation of the Lampedusa

High and the associated trough (Figure 5a). The profile features Lampedusa High flanked by a listric fault (between shot points 700 and 900), which reaches a depth of ~5.2 km (Figure 5a). In this area, the average thickness of the Lower Cretaceous stratigraphic unit is 2.3 km (Figure 5a). The Paleogene unit overlies the Cretaceous sediments, with an average thickness of a ~1 km depth profile. The overlying Tortonian-to-Messinian unit marked by shifting sea levels affecting sediment deposit has a thickness of ~0.7 km. The Plio-Quaternary unit caps the complete stratigraphic sequence, with a thickness of ~0.6 km (Figure 5a).

The ~1 km thick Lower Cretaceous sequence in the Western Linosa Graben is overlain by ~1 km Upper Cretaceous sediments (Figure 5b). The Paleogene and Tortonian-to-Messinian units follow the sequence upward, with ~1.3 km and ~1 km thickness, respectively. The top of the sedimentary fill is Plio-Quaternary, which has a maximum thickness of ~1 km in Figure 5b. The stratigraphic succession from Cretaceous to Plio-Quaternary appears interrupted by the volcanic bodies towards the Pantelleria Graben (Figure 5c). The Western Linosa Graben is deformed by a master planar normal fault dipping NW (approximately between shot points 2100 and 2300) [26]. The model locates the fault down to ~6 km depth (Figure 5b).

The stratigraphic unit thicknesses in (Figure 5a–c) are consistent with the interpretation described by Civile et al. (2021) [36], who defined a Plio-Quaternary succession 1.5 km thick in the main Linosa Graben. In our study, we determined the thickness of another part of the graben extending from SSE to NNW on the CS89-01 line, which is around 1.1 km (Figure 5b). For cross-checking this value, we assumed that the stratigraphy of the Riccio Sud-01 well is representative of the stratigraphy of the Lampedusa shelf, and we projected it on the modeled seismic profile (60 km to the NW). The depth-converted stratigraphic units (Figure 5a,e) and the stratigraphy reported in the well log show a good correspondence.

The above results show how the geological model can be improved by velocity modeling and consequent time-to-depth conversion of seismic horizons and faults of a raster/vintage seismic reflection profile. The velocity modeling dataset was used to reduce the uncertainties in the time-to-depth conversion, but still, the input dataset could be suitable if the seismic profiles are just available in scanned paper form and report the interval velocities of the CDP (Figure 3).

6. Conclusions

This study suggests that for an old, large-sized and noisy vintage seismic reflection profile in raster format, the velocity model building and depth conversion of horizons and faults from stacking velocities is a promising approach.

After multiple steps of interpolation of velocity values and time-to-depth conversion, the constructed depth profile provides a detailed image of the stratigraphic units and structural features found across the Sicily Channel from NNW to SSE. The velocity models and depth-converted seismic profiles provide overall insights into thegeological and structural information, like the thickness of different stratigraphic successions and the occurrence of volcanic bodies.

The availability of vintage seismic profiles helps researchers explore renewable energy sources at a lower cost than investing in modern subsurface data or conducting new surveys. Time-to-depth conversion of the horizons and faults of these vintage profiles through the smoothing of velocity models, as proposed in this study, is a requisite to gain cost-effective information for finding these energy and material resources during this transition time based on well/better-constrained subsurface geological models.

Supplementary Materials: The following supporting information can be downloaded at: https://www.mdpi.com/article/10.3390/geosciences15040114/s1, Supplementary Material S1: The Root Mean Square (RMS) or stacking velocities and interval velocities represented in the upper boxes (Figure 2a–c) associated with the respective time intervals were utilized for the calculation of depth. The SP* refers to the position of the Common Depth Point (CDP) gathers over which the stacking velocity analyses was carried out. Supplementary Material S2: Calculation of the depth of each stratigraphic horizon by following the relation: Thickness of individual layer = Interval velocity* (TWT base − TWT top)/2. Depth = sum of thicknesses for the individual layers. The interval velocities obtained after the application of Gaussian Convolution and data exclusion filters (Figure 4a–c) were used to calculate depth of each horizon at all CDP gathers to construct the depth profile (Figure 5a–c). Supplementary Material S3: (a–c) Inverse Distance Weighted (IDW) interpolation. (d–f) Kriging interpolation applied for the building of initial velocity models for three parts of the CS89-01 seismic line, which are also tested by Spline interpolation. The portions displayed with squares in (d–f) represent uncertain velocities. Both these interpolation methods are not suitable for generating good enough velocity models for further analysis (e.g., depth profile construction).

Author Contributions: Conceptualization, A.Q. and A.A.; methodology, A.Q. and A.A; software, A.Q.; validation, A.Q., A.A., N.C., M.M., A.S. and L.T.; formal analysis, A.Q., A.A., N.C., M.M., A.S. and L.T.; investigation, A.Q., A.A., N.C., M.M., A.S. and L.T.; data curation, A.Q., A.A., N.C., M.M., A.S. and L.T.; writing—original draft preparation, A.Q. and A.A.; writing—review and editing, A.Q., A.A., N.C. and M.M.; supervision, A.A. All authors have read and agreed to the published version of the manuscript.

Funding: This research is part of the PhD project of Aasiya Qadir granted by the Department of Chemistry, Life Sciences and Environmental Sustainability—University of Parma, Italy for the Earth Sciences PhD cycle number XXXVII a.a. 2021–2024 (Dottorandi | SCIENZE DELLA TERRA | Università di Parma).

Data Availability Statement: Data will be available upon request.

Acknowledgments: We sincerely acknowledge and thank the Department of Chemistry, Life Sciences and Environmental Sustainability—University of Parma, Italy, PhD project grant of Aasiya Qadir. We also sincerely acknowledge Eline Le Breton for the fruitful discussion, two anonymous reviewers for the insightful suggestions that improved the work and Muhammad Usman for his support.

Conflicts of Interest: The authors declare no conflicts of interest.

References

1. Diviacco, P.; Wardell, N.; Forlin, E.; Sauli, C.; Burca, M.; Busato, A.; Centonze, J.; Pelos, C. Data rescue to extend the value of vintage seismic data: The OGS-SNAP experience. *GeoResJ* **2015**, *6*, 44–52. [CrossRef]
2. Sopher, D. Converting scanned images of seismic reflection data into SEG-Y format. *Earth Sci. Inform.* **2018**, *11*, 241. [CrossRef]
3. Cicala, M.; Chiarella, D.; De Giosa, F.; Festa, V. Conventional data display and implications for the interpretation of seismic profiles: A discussion on the ViDEPI seismic database offshore Apulia (southern Italy). *Arab. J. Geosci.* **2022**, *15*, 395. [CrossRef]
4. Cicala, M.; De Giosa, F.; Piscitelli, A.; Scicchitano, G.; Festa, V. Conversion of vintage seismic reflection profiles of the ViDEPI dataset crossing the Gondola Line seismogenic fault (offshore Apulia, Adriatic Sea, Southern Italy) to SEG-Y. *Data Brief* **2024**, *55*, 110705. [CrossRef]
5. Diviacco, P.; Carlino, F.M.; Busato, A. Enhancing the value of public vintage seismic data in the Italian offshore. *Geosci. Data J.* **2019**, *6*, 6–15. [CrossRef]
6. Berra, F.; Stucchi, E.M.; Moretti, S. New information from "old" seismic lines: An updated seismic dataset for the northern Apennines. *J. Geophys. Eng.* **2019**, *16*, 215–225.
7. Maffucci, R.; Petracchini, L.; Livani, M.; Billi, A.; Carminati, E.; Cuffaro, M.; Petricca, P.; Doglioni, C. Seismic reflection profile dataset in a 3D environment of the northern Adriatic area. *Geophys. J. Int.* **2020**, *221*, 564–580.
8. Buttinelli, M.; Maesano, F.E.; Sopher, D.; Feriozzi, F.; Maraio, S.; Mazzarini, F.; Improta, L.; Vallone, R.; Villani, F.; Basili, R. Revitalizing vintage seismic reflection profiles by converting into SEG-Y format: Case studies from publicly available data on the Italian territory. *Ann. Geophys.* **2022**, *65*, DM538. [CrossRef]
9. Etris, E.; Crabtree, N.J.; Dewar, J. True depth conversion: More than a pretty picture. *CSEG Rec.* **2001**, *26*, 11–22.

10. Thore, P.; Shtuka, A.; Lecour, M.; Ait-Ettajer, T.; Cognot, R. Structural uncertainties: Determination, management, and applications. *Geophysics* **2002**, *67*, 840–852. [CrossRef]
11. Pon, S.; Lines, L.R. Sensitivity analysis of seismic depth migrations. *Geophysics* **2005**, *70*, S39–S42. [CrossRef]
12. Usman, M.; Siddiqui, N.A.; Garzanti, E.; Jamil, M.; Imran, Q.S.; Ahmed, L. 3-D seismic interpretation of stratigraphic and structural features in the Upper Jurassic to Lower Cretaceous sequence of the Gullfaks Field, Norwegian North Sea: A case study of reservoir development. *Energy Geosci.* **2021**, *2*, 287–297. [CrossRef]
13. Usman, M.; Siddiqui, N.A.; Zhang, S.Q.; Mathew, M.J.; Zhang, Y.X.; Jamil, M.; Liu, X.L.; Ahmed, N. 3D geo-cellular static virtual outcrop model and its implications for reservoir petro-physical characteristics and heterogeneities. *Petrol. Sci.* **2021**, *18*, 1357–1369. [CrossRef]
14. Sheriff, R.E.; Geldart, L.P. *Exploration Seismology*, 2nd ed.; Cambridge University Press: Cambridge, UK, 1995.
15. Yilmaz, Ö. *Seismic Data Analysis*; Society of Exploration Geophysicists: Tulsa, OK, USA, 2001; p. 2065. [CrossRef]
16. Bêche, M.; Kirkwood, D.; Jardin, A.; Desaulniers, E.; Saucier, D.; Roure, F. 2D Depth Seismic Imaging in the Gaspé Belt, a Structurally Complex Fold and Thrust Belt in the Northern Appalachians, Québec, Canada. In *Thrust Belts and Foreland Basins*; Springer: Berlin/Heidelberg, Germany, 2007; pp. 75–90.
17. Totake, Y.; Butler, R.W.; Bond, C.E. Structural validation as an input into seismic depth conversion to decrease assigned structural uncertainty. *J. Struct. Geol.* **2017**, *95*, 32–47. [CrossRef]
18. Miles, P.R.; Schaming, M.; Lovera, R. Resurrecting vintage paper seismic records. *Mar. Geophys. Res.* **2007**, *28*, 319–329. [CrossRef]
19. Conti, A.; Maffucci, R.; Bigi, S. The use of public vintage seismic reflection profiles: An example of data rescue from the eastern Tyrrhenian margin (Italy). In *Interpreting Subsurface Seismic Data*; Bell, R., Iacopini, D., Vardy, M., Eds.; Elsevier: Amsterdam, The Netherlands, 2022; pp. 127–156. [CrossRef]
20. Maiorana, M.; Sulli, A.; Marelli, M.; Agate, M. Geological characterization of a potential CO2 storage play in the Gela offshore (southern Sicily) and the role of a gravitational slide. *Mar. Petrol. Geol.* **2024**, *170*, 107127. [CrossRef]
21. Minissale, A.; Donato, A.; Procesi, M.; Pizzino, L.; Giammanco, S. Systematic review of geochemical data from thermal springs, gas vents and fumaroles of Southern Italy for geothermal favourability mapping. *Earth Sci. Rev.* **2019**, *188*, 514–535.
22. Civile, D.; Baradello, L.; Accaino, F.; Zecchin, M.; Lodolo, E.; Ferrante, G.M.; Markezic, N.; Volpi, V.; Burca, M. Fluid-Related Features in the Offshore Sector of the Sciacca Geothermal Field (SW Sicily): The Role of the Lithospheric Sciacca Fault System. *Geosciences* **2023**, *13*, 231. [CrossRef]
23. Scarascia, S.; LOZEJ, A.T.; Cassinis, R. Crustal structures of the Ligurian, Tyrrhenian and Ionian seas and adjacent onshore areas interpreted from wide-angle seismic profiles. *Boll. Geofis. Teor. Appl.* **1994**, *36*, 5–19.
24. Cassinis, R.; Scarascia, S.; Lozej, A. The deep crustal structure of Italy and surrounding areas from seismic refraction data; a new synthesis. *Boll. Soc. Geol. Ital.* **2003**, *122*, 365–376.
25. Torelli, L.; Zitellini, N.; Argnani, A.; Brancolini, G.; Cillia, C.; Peis, D.; Tricart, P. Sezione geologica crostale dall'avampaese pelagiano al bacino di retroarco tirrenico (Mediterraneo centrale). *Mem. Soc. Geol. Ital.* **1991**, *4*, 385–399.
26. Torelli, L.; Grasso, M.; Mazzoldi, G.; Peis, D.; Gori, D. Cretaceous to Neogene structural evolution of the Lampedusa Shelf (Pelagian Sea, Central Mediterranean). *Terra Nova* **1995**, *7*, 200–212. [CrossRef]
27. Argnani, A.; Torelli, L. Pelagian Shelf and its graben system (Italy/Tunisia). *Mem. Mus. Natn. Hist. Nat.* **2001**, *186*, 529–544.
28. Zarudzki, E.F.K. The Strait of Sicily. A Geophysical Study. *Rev. Geograph. Phys. Geo. Dynam.* **1972**, *14*, 11–28.
29. Winnock, E. Structure du Bloc Pelagien. In *Sedimentary Basins of Mediterranean Margins*; Wezel, I.F.C., Ed.; Tecnoprint: Bologna, Italy, 1981; pp. 445–464.
30. Finetti, I.R. Geophysical study of the Sicily Channel Rift Zone. *Boll. Geofis. Teor. Appl.* **1984**, *26*, 3–28.
31. Jongsma, D.; Van Hinte, J.E.; Woodside, J.M. Geologic structure and neotectonics of the North African continental margin south of Sicily. *Mar. Petrol. Geol.* **1985**, *2*, 156–179.
32. Reuther, C.D.; Eisbacher, G.H. Pantelleria rift-crustal extension in a convergent intraplate setting. *Geol. Rundsch.* **1985**, *74*, 585–597. [CrossRef]
33. Calanchi, N.; Colantoni, P.; Rossi, P.L.; Saitta, M.; Serri, G. The Strait of Sicily continental rift system: Physiography and petrochemistry of the submarine volcanic centres. *Mar. Geol.* **1989**, *87*, 55–83. [CrossRef]
34. Dart, C.J.; Bosence, W.J.; McClay, K.R. Stratigraphy and structure of the Maltese graben system. *J. Geol. Soc. Lond.* **1993**, *150*, 1153–1166. [CrossRef]
35. Civile, D.; Lodolo, E.; Accettella, D.; Geletti, R.; Ben-Avraham, Z.; Deponte, M.; Facchin, L.; Ramella, R.; Romeo, R. The Pantelleria Graben (Sicily Channel, Central Mediterranean): An example of intraplate "passive" rift. *Tectonophysics* **2010**, *490*, 173–183. [CrossRef]
36. Civile, D.; Brancolini, G.; Lodolo, E.; Forlin, E.; Accaino, F.; Zecchin, M.; Brancatelli, G. Morphostructural Setting and Tectonic Evolution of the Central Part of the Sicilian Channel (Central Mediterranean). *Lithosphere* **2021**, *2021*, 7866771. [CrossRef]
37. Maiorana, M.; Artoni, L.; Le Breton, E.; Sulli, A.; Chizzini, N.; Torelli, L. Is the Sicily Channel a simple Rifting Zone? New evidence from seismic analysis with geodynamic implications. *Tectonophysics* **2023**, *864*, 230019. [CrossRef]

38. Uyeda, S. Subduction zones: An introduction to comparative subductology. *Tectonophysics* **1982**, *81*, 3–4. [CrossRef]
39. Gueguen, E.; Doglioni, C.; Fernandez, M. On the post-25 Ma geodynamic evolution of the western Mediterranean. *Tectonophysics* **1998**, *298*, 259–269. [CrossRef]
40. Faccenna, C.; Funiciello, F.; Giardini, D.; Lucente, P. Episodic back-arc extension during restricted mantle convection in the central Mediterranean. *Earth Planet. Sci. Lett.* **2001**, *187*, 105–116. [CrossRef]
41. Faccenna, C.; Becker, T.W.; Lucente, F.P.; Jolivet, L.; Rossetti, F. History of subduction and back-arc extension in the central Mediterranean. *Geophys. J. Int.* **2001**, *145*, 809–820. [CrossRef]
42. Carminati, E.; Lustrino, M.; Doglioni, C. Geodynamic evolution of the central and western Mediterranean: Tectonics vs. igneous petrology constraints. *Tectonophysics* **2012**, *579*, 173–192. [CrossRef]
43. Van Hinsbergen, D.J.J.; Wissers, R.L.M.; Spakman, W. Origin and consequences of western Mediterranean subduction, rollback and slab segmentation. *Tectonics* **2014**, *33*, 347–595. [CrossRef]
44. Grasso, M.; Torelli, L. Cretaceous-Paleogene sedimentation patterns and structural evolution of the Tunisian shelf, offshore the Pelagian Islands (Central Mediterranean). *Tectonophysics* **1999**, *315*, 235–250. [CrossRef]
45. Argnani, A. The Strait of Sicily rift zone: Foreland deformation related to the evolution of a back-arc basin. *J. Geodyn.* **1990**, *12*, 311–331. [CrossRef]
46. Finetti, I.R.; Morelli, C. Geophysical exploration of the Mediterranean Sea. *Bull. Theor. Appl. Geophys.* **1973**, *15*, 263–340.
47. Finetti, I.R.; Del Ben, A. Crustal tectono-stratigraphic setting of the Pelagian foreland from new CROP seismic data. In *CROP PROJECT: Deep Seismic Exploration of the Central Mediterranean and Italy*; Finetti, I.R., Ed.; Elsevier B.V.: Amsterdam, The Netherlands, 2005; pp. 581–595.
48. Colantoni, P. Note di geologia marina sul Canale di Sicilia. *Giorn. Geol.* **1975**, *40*, 181–207.
49. Rotolo, S.G.; Castorina, F.; Cellula, D.; Pompilio, M. Petrology and geochemistry of submarine volcanism in the Sicily Channel. *J. Geol.* **2006**, *114*, 355–365. [CrossRef]
50. Argnani, A.; Cornini, S.; Torelli, L.; Zitellini, N. Diachronous foredeep-system in the Neogene-Quaternary of the Strait of Sicily. *Mem. Soc. Geol. Ital.* **1988**, *38*, 407–417.
51. Civile, D.; Lodolo, E.; Alp, H.; Ben-Avraham, Z.; Cova, A.; Baradello, L.; Accettella, D.; Burca, M.; Centonze, J. Seismic stratigraphy and structural setting of the Adventure Plateau (Sicily Channel). *Mar. Geophys. Res.* **2014**, *35*, 37–53. [CrossRef]
52. Calò, M.; Parisi, L. Evidences of a lithospheric fault zone in the Sicily Channel continental rift (southern Italy) from instrumental seismicity data. *Geophys. J. Int.* **2014**, *199*, 219–225. [CrossRef]
53. Ghisetti, F.C.; Gorman, A.R.; Grasso, M.; Vezzani, L. Imprint of foreland structure on the deformation of a thrust sheet: The Plio-Pleistocene Gela Nappe (southern Sicily, Italy). *Tectonics* **2009**, *28*, TC4015. [CrossRef]
54. Lodolo, E.; Civile, D.; Zanolla, C. Magnetic signature of the Sicily Channel volcanism. *Mar. Geophys. Res.* **2012**, *33*, 33–44. [CrossRef]
55. Micallef, A.; Geldmacher, J.; Watt, S.F.; Ferrante, G.M.; Ford, J.; Lodolo, E.; Civile, D.; Hodgetts, A.G.; Felgendreher, M.; Licari, J.G.; et al. Submarine volcanism in the Sicilian Channel revisited. *Mar. Geol.* **2024**, *474*, 107342.
56. Tesauro, M.; Kaban, M.K.; Cloetingh, S.A.P.L. EuCRUST-07: A new reference model for the European crust. *Geophys. Res. Lett.* **2008**, *35*, L05313. [CrossRef]
57. Milia, A.; Iannace, P.; Tesauro, M.; Torrente, M.M. Marsili and Cefalù basins: The evolution of a rift system in the southern Tyrrhenian Sea (Central Mediterranean). *Glob. Planet. Change* **2018**, *171*, 225–237. [CrossRef]
58. Grasso, M.; Pezzino, A.; Reuther, C.D.; Lanza, R.; Miletto, M. Late Cretaceous and Recent tectonic stress orientations recorded by basalt dykes at Capo Passer (south-eastern Sicily). *Tectonophysics* **1991**, *185*, 247–259. [CrossRef]
59. Grasso, M.; Lanzafame, G.; Rossi, P.L.; Schmincke, H.U.; Tranne, C.A.; Lajoie, J.; Lanti, E. Volcanic evolution of the island of Linosa, Strait of Sicily. *Mem. Soc. Geol. Ital.* **1991**, *47*, 509–525.
60. Biju-Duval, B.; Borsetti, A.M.; Colantoni, P. Geology of the troughs in the Strait of Messina-Tunisia, Pelagian Sea. Geologie des fosses du detroit siculo-tunisien (Mer Pelagienne). *Rev.-Inst. Fr. Du Pet.* **1985**, *40*, 691–722.
61. Jones, I.F. Estimating subsurface parameter fields for seismic migration: Velocity model building. In *Encyclopedia of Exploration Geophysics*; Society of Exploration Geophysicists: Houston, TX, USA, 2015; p. U1-1.
62. Dix, C.H. Seismic velocities from surface measurements. *Geophysics* **1955**, *20*, 68–86. [CrossRef]
63. Franke, R. Smooth interpolation of scattered data by local thin plate splines. *Comput. Math. Appl.* **1982**, *8*, 273–281.
64. Nwaila, G.T.; Zhang, S.E.; Bourdeau, J.E.; Frimmel, H.E.; Ghorbani, Y. Spatial interpolation using machine learning: From patterns and regularities to block models. *Nat. Resour. Res.* **2024**, *33*, 129–161.
65. Costa, J.C.; Schleicher, J. Double path-integral migration velocity analysis: A real data example. *J. Geophy. Eng.* **2011**, *8*, 154–161. [CrossRef]
66. Santos, H.B.; Schleicher, J.; Novais, A. Initial-model construction for MVA techniques. In Proceedings of the 75th European Association of Geoscientists and Engineers Conference and Exhibition 2013 Incorporating SPE EUROPEC 2013: Changing Frontiers, London, UK, 10–13 June 2013; pp. 2149–2153. [CrossRef]

67. Azubuike, I.M.; Akpan, B.N. Spline function as an alternative method to seismic data analysis. *Int. J. Stat. Appl.* **2017**, *7*, 36–42.
68. Cuevas, E.; Luque, A.; Escobar, H. Spline interpolation. In *Computational Methods with MATLAB®*; Synthesis Lectures on Engineering, Science, and Technology; Springer: Cham, Switzerland, 2024. [CrossRef]
69. Guan, S.; Biswal, B. Spline adaptive filtering algorithm based on different iterative gradients: Performance analysis and comparison. *J. Autom. Intell.* **2023**, *2*, 1–13.
70. Shekar, B.; Sethi, H. Full waveform inversion for microseismic events using sparsity constraints. *Geophysics* **2018**, *84*, KS1–KS12. [CrossRef]
71. Jiang, X.J.; Scott, P.J. Free-form surface filtering using wavelets and multiscale decomposition. In *Advanced Metrology 2*; Elsevier: Amsterdam, The Netherlands, 2020; pp. 195–246. [CrossRef]
72. Rointan, A.; Soleimani, M.M.; Aghajani, H. Improvement of seismic velocity model by selective removal of irrelevant velocity variations. *Acta Geod. Geophys.* **2021**, *56*, 145–176. [CrossRef]
73. Cabello, F.C.; León, J.; Iano, Y.; Arthur, R. Implementation of a fixed-point 2D Gaussian filter for image processing based on FPGA. In Proceedings of the 2015 Signal Processing: Algorithms, Architectures, Arrangements, and Applications (SPA), Poznan, Poland, 23–25 September 2015; pp. 28–33.
74. Agustina, I.; Nasir, F.; Setiawan, A. The implementation of image smoothing to reduce noise using Gaussian filter. *Int. J. Comput. Appl.* **2017**, *177*, 15–19. [CrossRef]
75. Rosie, A.M. *Information and Communication Theory*; Blackie: London, UK, 1966.
76. Rosin, P. Fitting superellipses. *IEEE Trans. Pattern Anal. Mach. Intell.* **2000**, *22*, 726–732.
77. Gries, D.; Schneider, F.B. Boolean expressions. In *A Logical Approach to Discrete Math*; Texts and Monographs in Computer Science; Springer: New York, NY, USA, 1993. [CrossRef]
78. Orsi, G.; Gallo, G.; Zanchi, A. Simple-shearing block resurgence in caldera depressions: A model from Pantelleria and Ischia. *J. Volcanol. Geotherm. Res.* **1991**, *47*, 2342931.
79. Sulli, A.; Calarco, M.; Agate, M.; Albano, L.; Bosman, A.; Di Grigoli, G.; Gargano, F.; Lo Presti, V.; Martorelli, E.; Pennino, V.; et al. Geohazard features of the north-western Sicily and Pantelleria. *J. Maps* **2024**, *20*, 2342931.
80. Rossi, P.L.; Tranne, C.A.; Calanchi, N.; Lanti, E. Geology, stratigraphy and volcanological evolution of the island of Linosa (Sicily Channel). *Acta Vulcanol.* **1996**, *8*, 73–90.
81. Distefano, S.; Gamberi, F.; Baldassini, N.; Di Stefano, A. Neogene stratigraphic evolution of a tectonically controlled continental shelf: The example of the Lampedusa Island. *Ital. J. Geosci.* **2019**, *138*, 418–431.